PAPER

Check for updates

Predictability of silver nanoparticle speciation and toxicity in ecotoxicological media†

Jan Köser, [iD] *[a] Maria Engelke,[a] Martin Hoppe, [iD] [b] André Nogowski, [iD] [c] Juliane Filser[a] and Jorg Thöming[a]

The use of silver nanoparticles (AgNPs) as an antimicrobial agent has increased significantly over the past decade which potentiates their release to the environment. The antimicrobial effect of AgNPs is generally considered to be due to the release of silver ions (Ag^+). Here we describe their bioavailability under environmental conditions and demonstrate its influence on (eco-)toxicity for the AgNP NM-300K and a wide variety of aquatic organisms (green algae, plants and crustaceans), terrestrial organisms (soil bacteria) and mammalian cells. Since the bioavailability of AgNPs is largely determined by Ag speciation, this paper focuses on the Ag speciation in the test media for these organisms. We predicted the Ag speciation in aqueous test media by equilibrium speciation calculation and validated the results by comparison with experimental speciation using ultracentrifugation and membrane filtration. Silver amounts were quantified using GF-AAS, ICP-OES/MS and UV-vis. The dissolved Ag concentrations were controlled by the fast initial release of a limited amount of Ag^+. After this initial release, the media components, chloride and proteins, controlled the available dissolved Ag by precipitation and complexation. Further release of Ag^+ due to oxidation was not observed in the time frame of our experiments, except for media with very high chloride content. Apparently, the stabilisers of these AgNPs prevented any further release accounting for an enhanced redox stability. These findings facilitated the prediction of the bioavailability of Ag in the test media and, based on literature toxicity data, also of its toxic effects (EC_{50}) on the respective organisms. The toxic effects of the AgNP NM-300K depended solely on the amount of Ag^+ that was already present in the stock dispersion and not from further release due to later oxidation processes.

Environmental significance

The OECD reference silver nanomaterial NM-300K was in the focus of many European joint research projects. Therefore, we studied its characteristics and their relation to the bioavailability and ecotoxicity of this particular nanomaterial in a wide variety of environmental media. NM-300K is very stable and behaves differently from commonly used silver nanoparticles. In conclusion, the observed toxic effects were only dependent on the amount of silver ions that was already present in the stock dispersion and not on the dissolution of NM-300K during the test. The presented results support the understanding of the behavior of NM-300K in various tests and environmental scenarios investigated throughout many European joint projects.

1 Introduction

Silver nanoparticles (AgNPs) are currently used in a broad variety of applications,[1] mainly due to their antimicrobial potential. There is a general consensus that the toxicity of AgNPs is largely determined by the release of Ag^+.[2]

[a] *UFT - Centre for Environmental Research and Sustainable Technology, University of Bremen, Leobener Straße 6, D-28359 Bremen, Germany.*
E-mail: koeser@uni-bremen.de
[b] *BGR - Federal Institute for Geosciences and Natural Resources, Stilleweg 2, D-30655 Hannover, Germany*
[c] *Technical University of Dresden, Institute of Process Engineering and Environmental Technology, D-01062 Dresden, Germany*
† Electronic supplementary information (ESI) available. See DOI: 10.1039/c7en00026j

In order to understand the toxicity of particulate silver materials like AgNPs and hardly soluble silver salts (*e.g.* $AgCl_s$ and Ag_2S_s), it is necessary to consider the speciation of silver in the test media and the amount of Ag^+ released into solution.[2–5]

Experimental speciation of silver in dispersions can be achieved by membrane filtration (MF)[6–10] or ultracentrifugation (UC)[3,6,8,9,11,12] and subsequent silver content measurement of the filtrate or supernatant in comparison with the untreated samples by *e.g.* atomic absorption spectroscopy (AAS),[6,9] inductively coupled plasma optical emission spectroscopy (ICP-OES) or mass spectrometry (ICP-MS).[7,9,11,12] These methods separate the sum of the dissolved silver species like Ag_{aq}^+, $[AgCl]_{aq}$, $[AgCl_2]_{aq}^-$ and complexes with organic

1470 | *Environ. Sci.: Nano*, 2017, **4**, 1470–1483

This journal is © The Royal Society of Chemistry 2017

molecules with low molecular weight (*e.g.* glutathione containing thiol groups) from the sum of the particulate silver species like AgNP, $AgCl_s$, Ag_2S_s and silver bound to large organic compounds like proteins and humic acids.

Another experimental speciation method is the measurement of plasmon resonance of AgNPs using ultraviolet and visible (UV-vis) spectroscopy and the calculation of the particle concentration *via* the Lambert–Beer relation, but this method discerns only the nanoparticulate form of silver from dissolved and other precipitated forms.[13,14] This method can also be used to calculate the mean particle size using Mie theory.[15,16]

Modern approaches for the characterisation of AgNPs include single particle ICP-MS (spICP-MS) and asymmetrical flow field flow fractionation (AF4) using *e.g.* ICP-MS as a detector.[17–19] These methods allow the determination of particle size, size distribution and major elemental composition of aqueous dispersions. The solid phase speciation of Ag for example in sludge can be done using X-ray absorption spectroscopy (XAS), specifically X-ray absorption near edge structure (XANES) and extended X-ray absorption fine structure analysis.[20,21]

The toxicity of Ag^+ has been investigated by several research groups for water-based species like *Daphnia magna*,[22] *Lemna minor*,[23] several algae species like *Pseudokirchneriella subcapitata* or *Chlamydomonas reinhardtii*[24] and the bacterium *Vibrio cholerae*.[25] The toxicity of AgNPs has been demonstrated *e.g.* for *Chlamydomonas reinhardtii*,[2,26] *Lemna minor*,[27] bacteria[28] and cells.[29]

Effective toxic concentrations were obtained for diverse aquatic organisms (*Daphnia magna*, *Lemna minor* and *Pseudokirchneriella subcapitata*) and for terrestrial organisms like *Arthrobacter globiformis* and *Eisenia andrei*.[30,31]

Depending on the test media composition and the sensitivity of the organisms, the effective concentrations of AgNPs and the most frequently used control $AgNO_3$ exhibit considerable differences which are shown for bacteria[30] and algae.[2,26] These results implied that the toxic effects were correlated with the concentration of Ag^+ released from AgNPs into the medium. In this context, one has to consider the influence of the changing environmental conditions during the life cycle on the AgNPs (*e.g.* in the aquatic environment). Prediction of the silver speciation should therefore enable the prediction of the toxic effects on the test organisms.

There have been several attempts to predict the chemical stability of AgNPs in environmental media and to predict silver speciation. In those studies, different software programs like *e.g.* visual MINTEQ (version 3.0),[32] MINEQL,[33] MINEQL+ (ver. 3.01)[34] and PHREEQC[35] were used.

Liu *et al.*[36] used thermodynamic analysis to predict the stability of AgNPs in water at different pH values and dissolved oxygen concentrations and found *e.g.* that the release rate was decreased with increasing pH or addition of humic or fulvic acids. The release of Ag^+ was measured and discussed for different media compositions[5,36] in terms of thermodynamic data of complex formation con-

stants for silver chloride complexes and the silver cysteine complex.

Fortin and Campbell[37] showed the influence of the chloride concentration on the speciation of silver. They found that the silver uptake by green algae *Chlamydomonas reinhardtii* was enhanced in the presence of silver chlorocomplexes.

Reinfelder and Chang[38] investigated the bioavailability of silver for the microalga *Thalassiosira weissflogii* in relation to the speciation of silver depending on the chloride concentration. The highest silver uptake was measured at the calculated maximum concentration of the species $[AgCl]_{aq}$. Jin *et al.*[39] calculated the theoretical maximum free Ag^+ concentration in synthetic "fresh water" matrices. Furthermore, they calculated the ionic strength, due to the fact that this property strongly affects the colloidal stability of electrostatically stabilised nanoparticle dispersions.[39] Levard *et al.*[40] discussed the environmental transformations of AgNPs and their impact on stability and toxicity. One major part dealt with the speciation of silver in environmental scenarios based on thermodynamic constraints. The authors stated that thermodynamic simulations represent a tool for the identification of potential environmental transformations of AgNPs, but interactions with complex organic matter and the kinetics can significantly change those predictions. They also identified the oxidation of metallic AgNPs as the starting point of any environmental transformation.

An approach to assess the long-term behavior of nanoparticles in test media by implementation of kinetic data into the model was proposed by Zhang *et al.*[7] and Liu *et al.*[36] for AgNPs in media that contain no chloride.

The goal of this work was to study the influence of the transformation of the reference nanomaterial NM-300K for the OECD sponsorship program[41] in environmental media on its ecotoxicity. This nanomaterial was in the focus of many European joint research projects[42,43] and of the joint research project UMSICHT.[44,45] For that purpose, we generated experimental and numerical speciation data of NM-300K in a large variety of media, compared them and used the outcome to explain the ecotoxicological effects of these AgNPs, which were determined in the context of UMSICHT.[44,45]

2 Materials and methods

2.1 Materials

The silver nanomaterial NM-300K (nominal diameter ≈15 nm, nominal silver content 10.16% (w/w), stabilised with 4% polyoxyethylene glycerol trioleate and 4% polyoxyethylene (20) sorbitan monolaurate in water (Tween-20)) was produced by ras materials (Regensburg, Germany) and provided by the Joint Research Center (JRC, Ispra, Italy).[41] Silver nitrate ($AgNO_3$, purum p.a., ≥99.0%) was purchased from Fluka (Buchs, Switzerland). The commercially available citrate stabilized AgNPs (NanoXact, nominal diameter 30 nm) were purchased from nanoComposix (San Diego, CA, USA). Nitric acid (puriss p.a., ≥99.0, 65%) was obtained from Sigma-Aldrich

This journal is © The Royal Society of Chemistry 2017

Environ. Sci.: Nano, 2017, **4**, 1470–1483 | 1471

(Munich, Germany) and hydrochloric acid (p.a., 37%) from VWR (Darmstadt, Germany). Palladium modifier (c(Pd) = 10.0 ± 0.2 g L^{-1} as Pd(NO$_3$)$_2$ in approx. 15% HNO$_3$) for graphite furnace atomic absorption spectroscopy (GF-AAS) was purchased from Merck (Darmstadt, Germany). Disposable tubes for sample preparation (15 mL & 50 mL, polypropylene (PP)) were obtained from Sarstedt (Nümbrecht, Germany), and pipette tips (2–200 μL & 50–1000 μL, PP) and tubes 1.5 mL (PP) for sample storage, digestion and dilution from Eppendorf (Hamburg, Germany). Sample cups (PP) for the autosampler were purchased from ThermoFisher Scientific (Dreieich, Germany). Argon (4.6, ≥99.996%) was obtained from Linde (Hamburg, Germany). Ultrafiltration devices (Vivaspin 500, PES, MWCO 3000) were purchased from Sartorius (Göttingen, Germany).

2.2 Preparation of nanoparticle dispersions

According to the procedures described by Klein et al.[41] the NM-300K dispersion (10.16%, w/w) was diluted to 2% (w/w) using MilliQ water. Immediately before further application, this stock dispersion was shaken vigorously and agitated using an ultrasonic bath for 15 min (Ultrasonic cleaner USC 100T, VWR, Darmstadt, Germany). A second stock dispersion was prepared directly before each set of experiments containing 1 g Ag L^{-1} in double distilled water (ddH$_2$O).

2.3 Determination of silver content by GF-AAS

Silver content was quantified by graphite furnace atomic absorption spectrometry (GF-AAS) using a Unicam 989 QZ AA spectrometer (Unicam, Cambridge, UK) with a GF-90 plus furnace and an FS-90 plus autosampler. *Aqua regia* digestion (HCl : HNO$_3$, 4 : 1, v : v) according the procedure reported in ref. 46 was chosen due to the wide range of chloride contents in the test media. The high excess of chloride prevents the precipitation of silver chloride (AgCl$_s$) and ensured the formation of soluble higher silver chloride complexes ([AgCl]$_{aq}$, [AgCl$_2$]$_{aq}^-$, *etc.*).[5,47]

2.4 Determination of silver content by ICP-OES/MS

Samples were digested using open vessel nitric acid digestion derived from the experimental setup of *aqua regia* digestion following the procedure described in the norm.[48] Digestion by nitric acid is an established method for silver and was earlier applied by Zhang *et al.*[7] Likewise Hagendorfer *et al.*[11] used nitric acid digestion and subsequent nitric acid dilution (with HNO$_3$ 1%, v/v) and concluded from clear and noncoloured solutions the complete mineralisation of AgNPs. In our study, the digestion was done by transferring the sample volume of 10 mL to the digestion vessel and adding 10 mL conc. HNO$_3$ (65%, w/w, Merck, Darmstadt, Germany). After heating to 130 °C, the sample was digested for 2 h. Subsequently, the samples were diluted with deionized water using a ratio of 1 : 5 (sample : water). Silver contents were then determined using inductively coupled plasma optical emission spectroscopy

(ICP-OES) (Ciros Vision, Spectro, Kleve, Germany). For silver concentrations below 500 μg L^{-1}, inductively coupled plasma mass spectroscopy (ICP-MS) (7500 series, Agilent, Böblingen, Germany) was used.

2.5 Quantification of dissolved silver content by membrane filtration (MF)

The dissolved silver content was determined by removing particulate silver (AgNPs or precipitated silver salts) using centrifugal ultrafiltration devices Vivaspin 500 containing PES membranes with a molecular weight cut off of 3 kDa. The manufacturer specifications describe the concentration of aprotinin ($M_w \approx 6512$) using Vivaspin 500 devices. Since the hydrodynamic diameter of aprotinin is ≈3 nm (ref. 49), the pore size of the membrane is estimated to be ≪3 nm. Filtration of samples was done by placing 500 μL in the ultrafiltration device prior to centrifugation for 30 min at ≈14 000 g using a MiniSpin plus centrifuge (Eppendorf, Hamburg, Germany). The filtrate was then digested and measured by GF-AAS as described below. No significant difference of direct measurement to membrane filtered samples was observed in the range from 10 μg Ag L^{-1} to 1.1 mg Ag L^{-1}, as shown in ESI† Fig. S4. Therefore, no significant sorption of Ag$^+$ to the membrane was assumed.

2.6 Quantification of dissolved silver by ultracentrifugation (UC)

An Optima L-100 XP from BeckmanCoulter (Krefeld, Germany), equipped with a Type 90 Ti rotor with a fixed angle, was used for UC. Centrifugation was performed in sealed tubes (12.5 mL, Polyallomer) at 80 000 rpm (≈400 000g) for 40 minutes. The calculated size cutoff for AgNPs under these conditions is approx. 3 nm using Stokes equation for sedimentation velocity and AgNP density (ρ_{Ag} = 10.5 g cm^{-3}).[11,50] The cutoff for proteins was estimated using density estimation for proteins $\rho \approx 1.36$ g cm^{-3}.[51] The cutoff size for proteins with the mentioned centrifugation conditions is then $M_w \approx 180$ kDa (diameter ≈ 8 nm assuming a spherical shape). Samples for measurement of silver content by ICP-OES/MS were taken from the centre of the centrifugation tubes with syringes (10 mL, PP, with a steel capillary attached).

2.7 Release experiments

Ag$^+$ release experiments were conducted in closed 15 mL (PP) tubes in three independent repeats with two replicates. The silver concentration was ≈10 mg L^{-1}. After placing 9.9 mL of test medium in each tube, a volume of 100 μL of the freshly prepared NM-300K stock dispersion with 1 g Ag L^{-1} was added. NM-300K at the same concentration in ddH$_2$O served as control. Please note that the media were prepared using ddH$_2$O equilibrated with air. The dissolved O$_2$ is therefore in excess to the Ag content (by factor ≈10, see section 2.10) ensuring comparability to the aeration of test media in most ecotoxicological experiments. After thorough mixing, the

1472 | *Environ. Sci.: Nano*, 2017, **4**, 1470–1483

This journal is © The Royal Society of Chemistry 2017

samples were stored in the dark at room temperature (20 °C). Samples for total silver content (GF-AAS) and for MF were taken after slight agitation after 2 h and at the end of the test period of the media related toxicity tests (2, 3 and 7 days, see section 2.8). For the UC, the release experiments were conducted with larger sample volumes of 50 mL to meet the minimum volume requirement for this method. Samples were prepared in 3 replicates, each consisting of 0.5 mL stock dispersion and 49.5 mL medium.

2.8 Test media composition, duration of release experiments and selected toxicity data

The test media chosen for the release experiments were used freshly prepared according to the following established test protocols. The selected test media and corresponding test organisms were in the focus of the joint research UMSICHT and were selected due to their environmental relevance and because they are representative for a variety of aquatic and terrestrial organisms and cells.[44,45] The corresponding toxicity data taken from the literature were determined in the context of the joint research project UMSICHT[31,44,45,52] (see Table 3). The EC_{50} values for Pseudok., Scened. and HepG2 (growth inhibition) were calculated as average ± standard deviation ($n = 3$).[44] The toxicity data for Arthrob. (enzyme activity inhibition) were calculated as median with 95% confidence limits ($n = 9$). The toxicity data for Daphnia (immobilisation) were calculated as average ± standard deviation for NM-300K ($n = 5$)[45] and for $AgNO_3$ as average ± 95% confidence limits ($n = 6$).[52] The toxicity data for Lemna (yield, dry weight) were calculated for NM-300K as geometric mean with 95% confidence intervals ($n = 3$)[31,45] and for $AgNO_3$ (growth rate, dry weight) as average ±95% confidence intervals ($n = 6$).[23]

Aquatic toxicity test media and experiment durations for this study were according to the following guidelines:

• Growth inhibition of green algae, *Pseudokirchneriella subcapitata*, OECD TG 201 medium,[53] duration of 3 days (d).

• Acute immobilisation inhibition of the water flea, *Daphnia magna*, Elendt M7 medium, OECD TG 202,[54] duration of 2 d.

• Growth inhibition of duckweed, *Lemna minor*, Steinberg medium, OECD TG 221,[55] duration 7 d.

• Growth inhibition of green algae, *Scenedesmus vacuolatus*, growth medium according to Matzke *et al.*[56] and Grimme & Boardman,[57] duration according to ref. 56 of 1 d, here 3 d.

Bacteria and cell toxicity test media and experiment durations for this study were according to the following guidelines:

• Solid contact test with soil bacteria, *Arthrobacter globiformis*, growth medium B composition for tests without soil according to Engelke *et al.*[30] modified from Neumann-Hensel & Melbye[58] and the standard protocol,[59] duration of 2 hours (h).

• Cell viability assay, HepG2 liver cell line, RPMI medium with 8% fetal calf serum (FCS) according to Arning *et al.*,[60] duration of 2 d.

The main components of the test media, the chloride and thiol group concentrations (see also section 2.10) and the ionic strengths are listed in Table 1. The detailed composition of the media is given in the ESI,† Table S4.

2.9 Determination of colloidal properties

Hydrodynamic diameters (HDD) were determined by dynamic light scattering (DLS) using a Beckman-Coulter DelsaNanoC (Beckman Coulter, Krefeld, Germany). The zeta potential was measured by electrophoretic light scattering (ELS), also using this device. Additionally, the plasmon resonance of the samples was recorded using a UV-vis spectral photometer (CADAS 200, Hach Lange, Berlin, Germany). These experimental methods are described in more detail in the ESI.†

2.10 Numerical speciation

The speciation of silver in test media was done numerically using PHREEQCi (v.3).[61] The database file *minteq.v4.dat* of the software[61] was used for the calculations since some amino acids and other organic components were already included in this database. Modifications to the database were applied to account for the complexation equilibria of cysteine with silver ions[13,62] and with the test media components magnesium, calcium, manganese, copper, zinc, iron and cobalt using the NIST standard database 46.8,[63] and data of Berthon *et al.*[64] and Goldberg *et al.*[65] The data for Ag^+–cysteine binding were also used to describe the binding of Ag^+ to

Table 1 Main components of the test media and durations of the tests, important reducing agents are marked **in bold** and oxidising agents are marked *in italics*. Ionic strengths were calculated using the software PHREEQCi (v.3).[61] The chloride and the thiol groups' contributions to the media are also given. The thiol group concentration was calculated using the approach with $n = 9$ available cysteine groups of BSA (see section 2.10). The detailed composition of the media is given in the ESI, Table S4

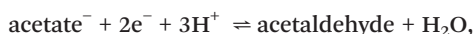| Organism (test medium)	Main components	Chloride [mM]	Thiol groups [mM]	Ionic strength [mM]	Test duration (d & h)
Lemna (Steinberg)	*KNO₃*, potassium phosphate buffer, *Ca(NO₃)₂*	0.01	—	9.3	7 d
Pseudok. (OECD TG 201)	NaHCO₃, **NH₄Cl**, CaCl₂, MgSO₄	0.65	—	1.7	3 d
Daphnia (Elendt M7)	CaCl₂, NaHCO₃, MgSO₄, *NaNO₃*	4.08	—	8.3	2 d
Scened. (algae growth)	NaCl, *KNO₃*, sodium phosphate buffer	8.25	—	25.4	3 d
Arthrob. (growth medium B)	NaCl, **glucose**, proteins	11.4	0.26	11.4	2 h
HepG2 (RPMI, 8% FCS)	NaCl, sodium phosphate buffer, NaHCO₃, **glucose**, KCl, amino acids, proteins	109.4	10.81	144.4	2 d

thiol groups in proteins.[5,13] A minor modification was done by omitting the silver chloride complex $[AgCl_4]_{aq}^{3-}$ from the equilibria calculations according to the study of Wood et al.[66] and Liu et al.[13]

$$Ag^+ + Cys^{2-} \rightleftharpoons [AgCys]^-, \log_{10} K_f = 11.9$$

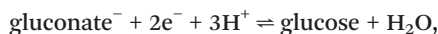$$Ag^+ + 2Cys^{2-} \rightleftharpoons [AgCys_2]^{2-}, \log_{10} K_f = 15.2$$

The binding of Ag^+ to proteins was approximated using the binding data for serum albumin. The binding data of Ag^+ with serum albumin reported by Shen et al.[67] and Zhao et al.[68] were considered in this work. Shen et al.[67] determined the interaction of Ag^+ with human serum albumin (HSA). They reported two binding sites (s and w) for the interaction of Ag^+ with HSA evaluated by the Scatchard-plot:[69] a strong interaction (s) with $\log_{10} K_s = -5.40$ with $n_s = 14$ sites and a weak interaction (w) with $\log_{10} K_w = -4.62$ with $n_w = 29$ sites (the selected values were reported for an intermediate HSA concentration of ≈ 1.4 g L^{-1}). Data reported from Zhao et al.[68] for a strong binding site of bovine serum albumin (BSA) to silver ions with $\log_{10} K_s = -3.69$ for $c_{Ag} \leq 1 \times 10^{-4}$ M was also evaluated here using a simplified approach with n set to unity.

Additionally, binding of Ag^+ with BSA was modelled using cysteine as a proxy for the available thiol groups of BSA. The number of exposed and therefore available cysteine groups of BSA was reported by Rombouts et al. ($n = 13$) and Alexander and Hamilton ($n = 9$).[70,71] All these different approaches to describe Ag^+ binding to proteins were compared to the experimental speciation data and are discussed in brief in section 3.4.

To account for possible redox reactions with test media components glucose and acetate, data of Thauer et al.[72] and Ramachandran et al.[73] (pK_α of gluconic acid = 3.7) were also included in the database. The dissolved oxygen content of the media was set to 8.3 mg L^{-1}, the solubility of O_2 in pure water at 25 °C and standard pressure.[61]

$$acetate^- + 2e^- + 3H^+ \rightleftharpoons acetaldehyde + H_2O,$$

$$\log_{10} K = 1.3438$$

$$gluconate^- + 2e^- + 3H^+ \rightleftharpoons glucose + H_2O,$$

$$\log_{10} K = 4.5723$$

The experimental speciation results of the MF of NM-300K in water (7.9 mg Ag L^{-1}, Ag_{aq}^+: 0.3 mg L^{-1}, Ag^0: 7.6 mg L^{-1}, see Fig. 1) were used as the initial conditions for the speciation calculations in the test media shown in Fig. 2.

3 Results & discussion

3.1 Determination of total silver content

A method comparison of GF-AAS, ICP-OES and evaluation of plasmon resonance was done in this study to ensure the reliability of the measurement of the total silver content. Two AgNP dispersions (NM-300K and NanoXact as nano material control) and $AgNO_3$ were used for this comparison. A nominal concentration of 20 mg Ag L^{-1} was chosen. The measurement of the AgNP containing dispersions gave ≈25% less than the nominal content independent of the used methods (ESI† Table S2). These results show that the actual silver content of the stock dispersions of NM-300K used in this study was lower than the nominal silver content of 10.16% (w/w). A long-term series of silver content measurements of NM-300K stock dispersions (each prepared freshly according section 2.2 from 9 different original vials) using ICP-OES and nitric acid digestion proved that the actual silver content was 79 ± 5% of the nominal content (ESI† Table S3).

Klein et al. reported ICP-OES results for the silver content of NM-300K with 9.2 ± 0.6% (w/w), which is also lower than the nominal value of 10.16% (w/w).[41] They discussed the influences of aging, sedimentation, formation of aggregates and adsorption in the vials as the possible causes for the silver content results. We confirm that occasionally the formation of aggregates was observed inside the vials. Supposing the aging of the sealed vials would increase the risk of adsorption and aggregate formation, one would expect a decrease of the measured silver contents. Our results contradict this expectation: we observed a steady slow increase of the silver content of the NM-300K vials over two years (ESI† Table S3). We suspect a loss of water in the vials due to slow diffusion through the fitting of the vials.

We determined the recovery of AgNPs in different media using the measured silver contents in the NM-300K vials as reference. The application of the described GF-AAS method using modified aqua regia revealed a satisfactory average recovery of 97 ± 4% of Ag for NM-300K for the wide variety of test media studied here (ESI† Fig. S3), with no significant differences between these.

3.2 Colloidal properties of NM-300K

The colloidal properties of the AgNPs in the test media were checked in the time frame of the tests in separate experiments using dynamic light scattering and electrophoretic light scattering.[44] Additionally, UV-vis spectra were recorded in the same time frame.[44] Briefly, the NM-300K were colloidally stable in all media investigated here. For most media, the hydrodynamic diameter was in the range of 30–60 nm. For some of the media, slight agglomeration was observed, but that did not lead to sedimentation (Daphnia, Algae growth and HepG2 medium). The zeta potential of NM-300K in water (pH 7) was in the range of −15 to −25 mV; in the other investigated test media, the zeta potential ranged from approx. 0 to −25 mV (the pH in the test media ranged from

1474 | Environ. Sci.: Nano, 2017, 4, 1470–1483

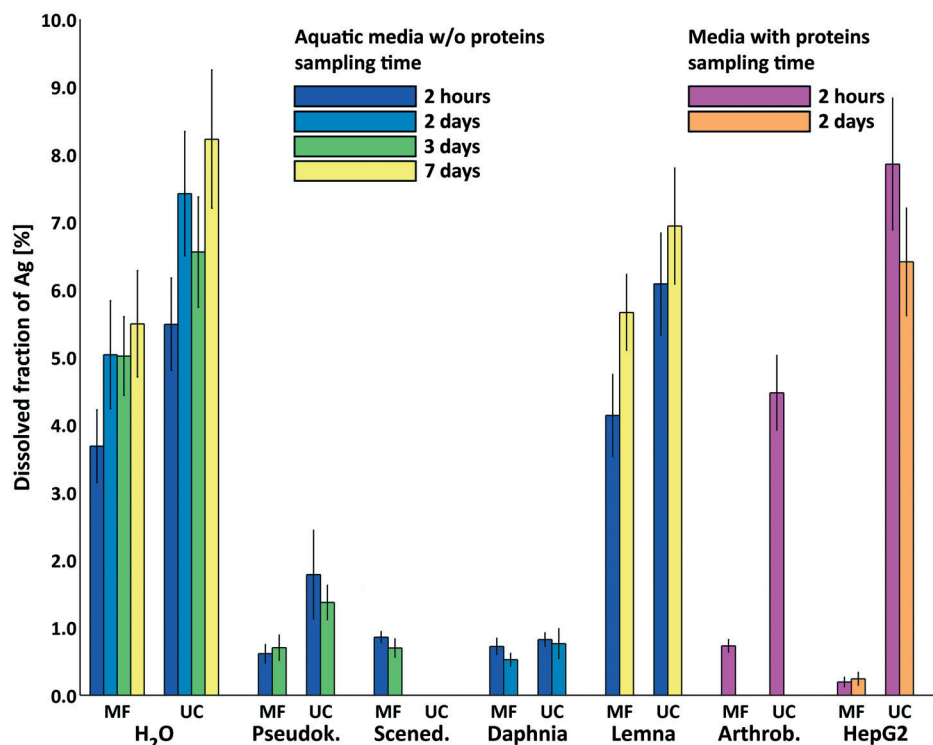This journal is © The Royal Society of Chemistry 2017

Fig. 1 Dissolved silver fraction in test media determined using ultrafiltration membranes (MF) and ultracentrifugation (UC) after 2 hours (left column of each group) and at the end of the ecotoxicological tests (2, 3 and 7 days, respectively, see section 2.8 and Table 1) (right column of each group). The results for aquatic test media are displayed in the center of the plot (coloured blue to yellow). Measurements for medium water were performed at all time points of the tests (2 hours, 2, 3 and 7 days). Note that media for Arthrobacter (test duration 2 hours) and HepG2 (coloured pink and orange) contain proteins. Data are shown as mean ± standard deviation with $n \geq 3$ except for 2 h $MF_{Pseudok.}$ and $MF_{Scened.}$ $n = 2$ (NM-300K AgNP @7.9 mg Ag L^{-1}).

pH 6 to 8). The results are given in more detail in the ESI,† Fig. S5–S7. The colloidal stability was attributed to the strong steric stabilisation of the AgNPs with polyoxyethylene glycerol trioleate and Tween-20.

3.3 Experimental silver speciation

We measured the released Ag^+ in the biological test media, because the toxicity of AgNPs for organisms is largely determined by the release of Ag^+.[2] In Fig. 1, the silver releases are shown for NM-300K dispersions (7.9 mg Ag L^{-1}) in different biological test media determined by both MF and UC. The releases were less than $\approx$8% and clearly showed significant differences between the test media. The results were consistent for MF and UF except for media containing proteins.

In media without proteins and very little chloride (H_2O and Lemna medium), the initial dissolved silver fraction was high (MF: both media $\approx$4% and UC: both media $\approx$6% each after 2 hours). For the AgNPs in water samples, the released silver increased to $\approx$5% (MF) and $\approx$7% (UC) after 2 days. The measurements after 3 and 7 days showed no further significant increase of silver release. These results indicate the equilibration of both AgNPs and dissolved silver in the samples. A similar behavior of only partial dissolution of AgNPs in pure water in the presence of air was reported by Kittler

et al.[10] and Loza et al.[74] The released silver in Lemna medium after 7 days was similar to the corresponding results in water at the same time point. Loza et al.[74] ascribed the dissolution of AgNPs to the dissolved O_2 in the media, which also appears to be the general agreement in the literature. The rate and extent of dissolution of AgNPs strongly depend on their size, shape and coating and on the composition of the medium.[13,74] In addition to that, complete dissolution of AgNPs is seldom achieved by molecular O_2; in many cases a stronger oxidation agent like H_2O_2 is necessary for complete dissolution.[74]

Liu et al.[5] concluded that O- and N-rich polymer coatings can both delay and extend ion release by accumulating and releasing surface-bound Ag^+. Considering that high concentrations of polyoxyethylene glycerol trioleate and Tween-20 were used as stabilisers for NM-300K, we suggest that some Ag^+ was already present in the stock dispersion of NM-300K bound to these stabilisers. The stabilisers acted probably as a fast releasing reservoir for Ag^+ and had the additional effect of later hindering the access of O_2 to the AgNP surface. This would explain the characteristic Ag^+ release behavior determined in our release experiments in water and Lemna medium.

Therefore, we suggest as a realistic approach setting the initial conditions for speciation calculations to the initial
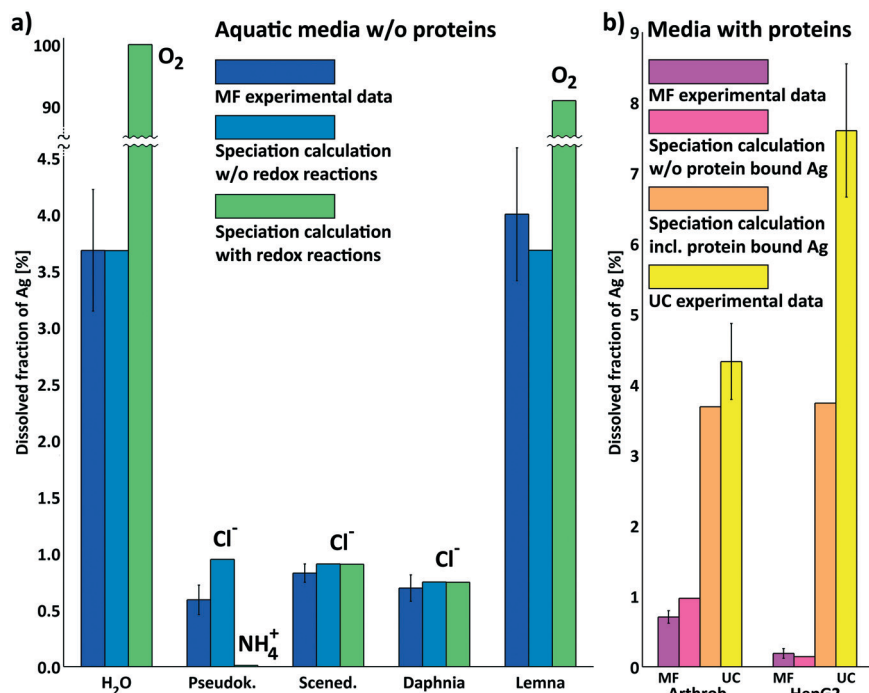
Fig. 2 Comparison of experimental (by MF) *vs.* speciation calculated dissolved Ag in the test media for NM-300K AgNPs@7.9 mg Ag L^{-1}. a) Comparison for media without proteins: the experimental data (MF) are represented by the leftmost column in each group. The speciation calculation was done without allowing for possible redox reactions (central column in each group) and with allowing for redox reactions (rightmost column in each group). The controlling medium component is given at the top of the respective bars. b) Protein effect on Ag speciation in test media for Arthrobacter and HepG2. Experimental data for membrane filtration (MF) are represented by the leftmost column and for ultracentrifugation (UC) rightmost column. The inner columns represent results for speciation calculation (without allowing for redox reactions) for dissolved silver not bound to proteins (inner left) and total dissolved silver (dissolved and bound to proteins) (inner right) (with n = 9 available cysteine groups of BSA).

composition of the experiment with water (total Ag 7.9 mg L^{-1}, Ag$_{aq}^+$ 0.3 mg L^{-1} and Ag^0 7.6 mg L^{-1}) and conducting the speciation calculations as a two-stage process. This would resemble the processes that we observed and were similarly reported by Liu *et al.*[5] for AgNPs pretreated with O$_3$ showing a fast initial release of Ag$^+$ already present in the beginning (for NM-300K as Ag$^+$ bound to stabilisers and for the O$_3$-pretreated AgNPs as Ag$_2$O on the AgNP surface) and as a second step accounting for the influence of redox reactions like the later slow increase of dissolved silver by metal-dioxygen reaction in the test solutions.

In media with higher chloride contents (Pseudok., Scened. and Daphnia medium), the dissolved silver fractions were in the range of 0.5% to 2%. No increase of dissolved silver was obtained over time from 2 hours to 2 or 3 days. A similar release behavior was reported by Li and Lenhart[75] for Tween-80 coated AgNPs in Olentangy river water with 2.2 mM chloride concentration. They found ≈2.5% of released Ag$^+$ after 6 h with no further increase over time (15 days) in the medium. In contrast, for bare AgNPs and citrate coated AgNPs, they reported a slow increase of the dissolved silver over time. This suggests that part of the released Ag$^+$ was already present in the nanoparticle stock dispersion probably bound to the coating material Tween-80 and also supports our two-stage approach for the speciation calculations.

The dissolved silver fraction determined by MF for Arthrob. medium was 0.7%. In contrast, the dissolved silver fraction by UC was, at 4.3%, significantly larger. This difference of both separation methods was particularly pronounced for the HepG2 medium with ≈0.2% by MF and ≥6% by UC. The discrepancy can be explained by (a) the binding of Ag$^+$ to the thiol groups of proteins in the media[13] and (b) the differences in cutoff sizes of the methods MF and UC. The cutoff sizes for the method UC were estimated for AgNPs to be ≈3 nm and for proteins to be ≈180 kDa (see section 2.6). For the MF method, the cutoff sizes were smaller: for AgNPs ≪3 nm estimated and for proteins ≪3 kDa (see section 2.5). Ag$^+$ bound to proteins were therefore separated by MF, whereas they stayed in the supernatant with UC and contributed to the dissolved Ag$^+$ fraction.

This behavior was observed for the HepG2 medium with FCS. A high fraction of the FCS, that consists mainly of bovine serum albumin (BSA) with a molecular weight of 69.3 kDa,[76] was separated by MF. Meanwhile, the cutoff of the UC method was much higher and thus the main part of proteins was left in the supernatant. For the Arthrob. medium, a similar behavior was measured. This was expected, because a high fraction of the protein components casein, peptone and yeast extract of the medium have molecular weights >1 kDa (≈10–40%, *e.g.* (ref. 77)).

1476 | *Environ. Sci.: Nano*, 2017, **4**, 1470–1483

This journal is © The Royal Society of Chemistry 2017

The silver releases of the water, Lemna medium and Pseudok. medium samples were slightly higher for UC than for MF (see Fig. 1). These findings can also be related to the different cutoff sizes of both methods. Small AgNPs near the cutoff size of the UC method (3 nm) could cause a slightly higher apparent silver release. These results were in accordance with the results of Klein et al.[41] Data based on TEM images revealed that the average particle size was 15 nm, but also a second smaller particle fraction at 5.4 nm could be observed.

Similar results were obtained by Unrine et al.[8] for the comparison of UC and MF separation. They reported that MF gave generally lower dissolved silver contents and that some of the smaller AgNPs (<4 nm) were probably not removed by UC, when moderate centrifugation conditions were used. They also discussed that the humic or fulvic substances from aquatic sources could be removed by MF (3 kDa) but not by UC, because they were smaller than the cutoff of the UC method (7–10 nm) and therefore stayed in the supernatant after UC. This corresponds to our findings for media containing proteins. For dispersions with higher solid content of approx. 10%, Zirkler et al.[78] reported differences of MF and UC and offered pore clogging or the formation of filter cake as an explanation. This could be excluded considering the very dilute media used here.

The results for silver release in Daphnia medium differed from the findings for the other described media. There were no significant differences between MF and UC. This medium contains more chloride (4.08 mM) compared to Lemna medium (10 μM), Pseudok. medium (0.65 mM) and pure water. The slightly higher chloride content could be responsible for the faster dissolution of small AgNPs in Daphnia medium, due to the decreased chemical stability of AgNPs.[40,79] In media with low chloride content, these very small AgNPs were separated by MF, causing the difference with the UC results.

In summary, the most important components for the silver speciation were chloride and thiol containing proteins (besides O_2) due to their strong binding to Ag^+, which was also reported for other AgNPs by many other groups like Liu et al.[13] and Levard et al.[40]

3.4 Speciation calculations of AgNPs in test media

Speciation calculations were conducted to discuss the outcome of our release experiments and to check which approach was suitable to predict the silver speciation in toxicological test media. We did speciation calculations for the theoretical maximum concentrations of dissolved silver, discussed the influence of reducing and oxidising components on silver speciation in the media and the binding of Ag^+ to chloride and proteins.

The theoretical maximum concentrations of dissolved silver ($[Ag^+]_{max}$) in the test media (see in Table 2) were calculated using PHREEQCi according to Jin et al.[39] and Loza et al.[74] (see section 2.10). The calculations were done by increasing the Ag^+ concentration until precipitation started as indicated by the software. The Pseudok., Daphnia and Scened. media contain higher amounts of chloride and no proteins. Hence, the $[Ag^+]_{max}$ values were close to the experimentally determined values with MF. Li and Lenhart[75] also reported dissolved silver concentrations that are relatively close to the theoretical maximum concentration of ≈57 μg L^{-1} in Olentangy river water, when taking only the inorganic components of the river water into account. For the Lemna medium, $[Ag^+]_{max}$ was much higher than the experimental values. This was probably caused by the Ag^+ release of NM-300K reaching equilibrium conditions before $[Ag^+]_{max}$.

For the Arthrob. medium, the $[Ag^+]_{max}$ corresponded well with the UC speciation data because of Ag^+ binding to thiol groups of the proteins in the medium (calculated with the BSA approach with $n = 9$ available cysteine groups, see section 2.10). For HepG2 medium, the $[Ag^+]_{max}$ is much higher than the experimental speciation data, which was probably also caused by the Ag^+ release of NM-300K reaching equilibrium conditions before $[Ag^+]_{max}$.

Our first approaches were done to figure out if a simple equilibrium speciation calculation approach would lead to realistic predictions. We calculated the equilibrium conditions of the AgNP/medium mixtures without any restrictions, in this way including redox reactions. These first calculations considered the nominal Ag concentration of 10 mg Ag L^{-1} as the reduced form Ag^0 (corresponding to 93 μmol L^{-1}). For the media without reducing components (NH_4^+ and glucose), these calculations led to total oxidation of Ag^0 to Ag^+ because dissolved O_2 in the media was present in excess (8.3 mg L^{-1} or 0.26 mM, see also section 2.10). In the presence of NH_4^+ or glucose (Pseudok., Arthrob. and HepG2 media), the calculations led to almost all silver present in the reduced form Ag^0 (see the detailed compositions in the ESI,† Table S4). The

Table 2 Comparison of dissolved silver in the media. The predicted maximum dissolved silver concentrations $[Ag^+]_{max}$ and the measured concentration values by MF and UC at day 0 are given (as mean ± standard deviation, $n \geq 3$ except for $MF_{Pseudok.}$ and $MF_{Scened.}$ $n = 2$). Additionally, the chloride content and the approximated thiol group concentration in the media are listed (using BSA with $n = 9$ available cysteine groups, see section 2.10)

Organism (test medium)	Chloride [mM]	Thiol groups [mM]	$[Ag^+]_{max.}$ [μg L^{-1}]	Ag_{MF}^+ [μg L^{-1}]	Ag_{UC}^+ [μg L^{-1}]
H_2O	0.0	—	—	291 ± 43	434 ± 54
Lemna (Steinberg)	0.01	—	2370	317 ± 47	465 ± 58
Pseudok. (OECD TG 201)	0.65	—	74	47 ± 1	136 ± 50
Daphnia (Elendt M7)	4.08	—	58	55 ± 9	63 ± 8
Scened. (algae growth)	8.25	—	71	65 ± 6	—
Arthrob. (growth medium B)	11.4	0.26	302	56 ± 7	342 ± 43
HepG2 (RPMI, 8% FCS)	109.4	10.81	1940	15 ± 5	601 ± 75

This journal is © The Royal Society of Chemistry 2017

Environ. Sci.: Nano, 2017, 4, 1470–1483 | 1477

same outcome was observed when considering 10 mg Ag L^{-1} as the oxidised form of Ag^+ as the starting conditions, because the redox active components O_2, NH_4^+ and glucose were in excess related to the silver in the media. These first calculation results giving either total oxidation of Ag to Ag^+ or almost total reduction to Ag^0 clearly did not represent the outcome of our release experiments shown in Fig. 1.

Therefore, we decided to conduct the speciation calculations in two subsequent steps as suggested by our experimental results following Liu et al.[5] and Li and Lenhart.[75] This was considered by setting the starting conditions of the calculations to the experimentally determined speciation after the fast initial release of Ag^+ from the stabilisers. The first step calculations allowed only for dissolution, precipitation and complexation equilibria. These were assumed as fast processes in the time frame of the studied toxicity tests. The constraint in this first step was not allowing for redox reactions. The second step was relaxing the constraint conditions and was allowing for redox reactions, which accounted for the then predominant slow metal-dioxygen reaction.[5] Since the tested dispersions were prepared from NM-300K/H_2O stock dispersions, it was straightforward to estimate the speciation in test media using the initial experimental speciation in water (MF, 2 h) as the initial conditions.

In Fig. 2a the calculation results of these two steps are shown in comparison with the experimental results for NM-300K in media without proteins separated by MF (after 2 h). The first step calculations correctly predicted the available dissolved silver content in the test media in the time frame of the tests. The initial speciation in H_2O is crucial for the bioavailability of dissolved silver in the tests.

The results show that the available Ag^+ was controlled by the chloride content of the media. For media with higher chloride content (Pseudok., Scened. and Daphnia medium), the initial amount of Ag^+ was reduced by chloride by precipitation of $AgCl_s$. For the media with very low chloride (H_2O and Lemna), the initial amount of Ag^+ was still available because no precipitation as $AgCl_s$ occurred. This was shown by the good concordance of experimental results and the first step calculations not allowing for redox reactions hinting that redox reactions played only a minor role within the time frame of the tests. This was also supported by the results of Li and Lenhart for silver release of Tween-80 coated AgNPs.[75]

Second step calculations allowing for redox reactions estimated the long term behavior and the direction of the processes to either oxidative dissolution or stabilisation of AgNPs. The amount of O_2 in the calculated systems led to complete oxidation and total release of Ag^+. For the media (H_2O and Lemna) this was clearly shown in Fig. 2a in the rightmost bars for H_2O and Lemna medium with values for dissolved silver above 90%. This extreme increase was in the same direction of the trend of experimental data for MF in Fig. 1 for H_2O and Lemna medium. The second step calculations for Scened. and Daphnia medium (containing 8.25 mM and 4.08 mM chloride, respectively) led to complete oxidation with dissolved O_2 of all the initial Ag^0 to Ag^+ as explained ear-

lier in this section. However, the higher chloride content led to precipitation of the additional released Ag^+ from oxidation as $AgCl_s$ and thus still controlled the available dissolved silver.

Reducing components such as ammonium (Pseudok. medium) and glucose (Arthrob. and HepG2 medium) were in excess to dissolved O_2 and the initial amount of Ag^+ and led to almost complete reduction of Ag^+ to silver metal Ag^0. This was not in agreement with the experimental findings, which was probably related to the restriction to the moderate temperature of 25 °C in this study and the usually very slow reduction reactions involving NH_4^+. The silver mirror reaction (Tollens' reagent for the aldehyde test) for example needs elevated temperatures to work (e.g. heating over Bunsen burner flame). Data reported by Khan et al.[80] showed a decrease in the rate of Ag^+ reduction in the presence of ammonia ($c_{NH_3} < 3$ mM) due to formation of silver ammonia complexes, indicating its more important role as a complexing agent with a similar effect reported for chloride.[40] Dissolution experiments of AgNPs in the presence of glucose reported by Loza et al.[74] show only a decelerating effect of glucose on the Ag^+ release. Nevertheless, the final release was similar to the AgNPs in water without glucose. This also supports the minor role of glucose as a reducing agent in the discussed media.

In Fig. 2b experimental and speciation calculation results are compared for the media containing proteins. For these media, the experimental results for MF corresponded to the results of the speciation calculation for dissolved Ag^+ not bound to proteins. The experimental results for UC also matched the results of the speciation calculations for dissolved Ag^+ including the Ag^+ bound to proteins. For HepG2 medium, the experimental outcome for UC was higher than the numerical result for Ag^+ bound to proteins and amino acids, probably because the very high chloride content (109 mM) caused further release of Ag^+ by accelerating the oxidative dissolution of AgNPs as reported in ref. 40. Speciation calculation results with allowing for redox-reactions are not shown in this figure.

The numerical approach supports that the differences between the results for MF and UC for media containing proteins were caused by the binding of Ag^+ to proteins that were not separated by UC (<180 kDa), but were separated by MF (>3 kDa). Considering the good concordance of the experimental and numerical results, the binding of Ag^+ to proteins was modeled nicely following Liu et al. using the data for Ag^+ binding to cysteine and the number of exposed cysteine groups of BSA reported by Rombouts et al. ($n = 13$) and Alexander and Hamilton ($n = 9$)[13,70,71] considering only first step calculations without allowing for redox reactions. The number of available cysteine groups of BSA $n = 9$ was used for the data represented in Fig. 2b. The different approaches to model Ag^+ to protein binding given in section 2.10 were compared regarding the absolute of the $\log_{10}$ of the relative deviation of the calculated from the experimental Ag^+ concentration. The experimental speciation data was well represented

1478 | Environ. Sci.: Nano, 2017, 4, 1470–1483

This journal is © The Royal Society of Chemistry 2017

Table 3 Experimental EC$_{50}$ values (± standard deviation) for NM-300K and AgNO$_3$ from the literature for the test organisms related to the here investigated test media; data in ()-parentheses represent the confidence limits (95%) of the EC$_{50}$ determination. Details on the selection and the calculation of the cited EC$_{50}$ values are given in section 2.8. Additionally, the predicted dissolved Ag concentrations from speciation calculations at NM-300K EC$_{50}$ in the test media are given

Test organism	EC$_{50,\text{NM-300K}}$ [µg Ag L^{-1}]	Calc. Ag$_{\text{diss}}^+$ at EC$_{50,\text{NM-300K}}$ [µg Ag L^{-1}]	EC$_{50,\text{AgNO}_3}$ [µg Ag^{-1}L]
Pseudok.	617 ± 367 (ref. 44)	22.7 ± 13.5	16.1 ± 4.9 (ref. 44)
Scened.	1399 ± 540 (ref. 44)	51.4 ± 19.9	8.4 ± 3.2 (ref. 44)
Daphnia m.	41 ± 14 (ref. 45)	1.5 ± 0.5	2.3 ± 0.3 (ref. 52)
Lemna m.	496 (192 1105)[31]	18.2 (7.1 41)	31 (26 37)[23]
Arthrob.	33 380 (29 940 38 370)[30]	233 (233 233)	1430 (1210 1710)[30]
HepG2	≫50 000 (ref. 44)	≫1839	7080 ± 2410 (ref. 44)

by the BSA approach with $n = 9$ and $n = 13$ available cysteine groups (see also ESI† Table S6).

3.5 Prediction of AgNP toxicity (EC$_{50}$) based on silver speciation

Considering the consensus that AgNP toxicity is largely determined by the released Ag$^+$,[2] it is straightforward to base a prediction of AgNP toxicity on the speciation of the released Ag$^+$ within the tests. In Table 3 toxicity data from the literature as EC$_{50}$-values (± standard deviation or with confidence limits (95%) given in ()-brackets) were listed for the organisms, which correspond to the investigated test media, for AgNPs (NM-300K) and AgNO$_3$. The corresponding toxicity data taken from the literature were determined in the context of the joint research project UMSICHT[31,44,45,52] (see also Table 3 and EC$_{50}$ calculation details in section 2.8).

Experimental NM-300K EC$_{50}$ in the second column were used as total Ag concentrations (initial composition Ag^0 fraction 96.3% and Ag$^+$ fraction 3.7% as described in section 2.10) present in the media for calculating the dissolved Ag concentrations (third column) without allowing for redox-reactions (first step speciation calculations according to our approach, see section 2.10). The results of these speciation calculations are shown in the ESI† in Fig. S8–S12 except for HepG2. The figures show also the change of speciation of Ag with the change of dosage of NM-300K to the media resembling the typical toxicological effect–concentration plots. Additionally, speciation calculations were conducted to visualise the change of speciation of Ag with the addition of AgNO$_3$ to the media for Arthrobacter and HepG2 (in Fig. 4 and in the ESI† in Fig. S13 & S14). For all media, the Ag$^+$-concentrations at the EC$_{50}$ were below the maximum dissolved Ag$^+$-concentration (Table 2) and no precipitation was predicted except for the Arthrobacter medium. Here the speciation calculations predicted precipitation of most of the Ag$^+$ as AgCl$_s$.

Surprisingly, the comparison of these calculated data with experimental AgNO$_3$ EC$_{50}$ (fourth column) shows good agreement. This suggests that it is possible to reversely predict NM-300K EC$_{50}$ when using AgNO$_3$ EC$_{50}$ as estimated dissolved Ag concentration values. The experimental AgNO$_3$ EC$_{50}$ values were then used as initial Ag$^+$ concentrations for the prediction of NM-300K EC$_{50}$. As a result, the predicted

NM-300K EC$_{50}$ shows excellent agreement with the experimentally determined values (see Fig. 3). In this figure, the toxicity data for *Desmodesmus subspicatus*, *Danio rerio* and *Myriophyllum spicatum* are also shown and were used to test our prediction approach[45] (listed in ESI† Table S4). In all but one case, the deviation is in the range of the experimental standard deviation (or the confidence interval). This is even the case for Arthrobacter when considering the contribution of colloidal AgCl$_s$ to the toxic effect. The change of Ag speciation with the dosage of AgNO$_3$ in the Arthrobacter medium with the inhibition data of Engelke et al.[30] is shown in Fig. 4. The experimental EC$_{50}$ of 1.43 mg Ag L^{-1} is in the concentration range $c_{\text{Ag}} > 2 \times 10^2$ µg Ag L^{-1}. In this range the speciation calculation predicted no increase of total dissolved Ag$^+$ and only the amount of precipitated AgCl$_s$ increased. Therefore, it was very clear that bioavailable AgCl$_s$ contributed to the toxic effect in this test. We suppose that the precipitated AgCl$_s$ is bioavailable because of colloidal stabilisation due to the proteins present in the test medium. A similar behavior was described by Loza et al. for Ag$^+$ in test media for bacteria and cells.[81]
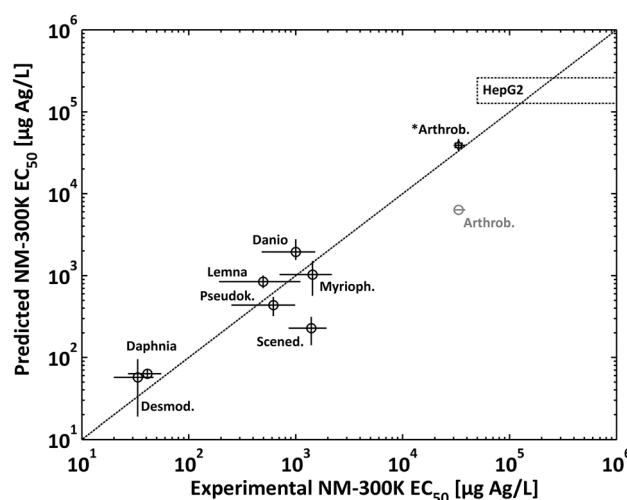
Fig. 3 Comparison of experimental EC$_{50}$ values with predicted EC$_{50}$ for NM-300K. For *Arthrobacter the prediction also considers the colloidal species AgCl$_s$ (see Fig. 4). In the case of HepG2 only the lower limit of the EC$_{50}$ could be determined experimentally (dotted rectangular, see text).
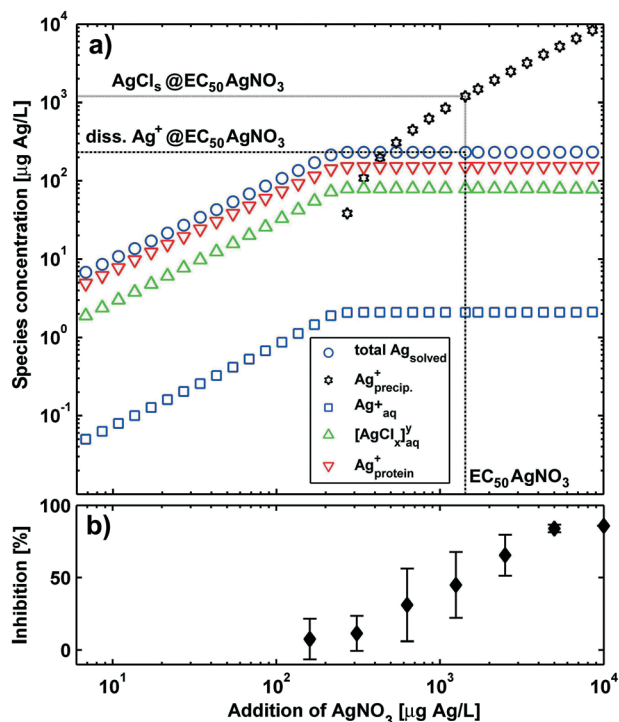
Fig. 4 Comparison of a) silver speciation of $AgNO_3$ in growth medium for Arthrobacter with b) the experimental toxicity data for $AgNO_3$.[30] The dotted line represents the data for the EC_{50} of $AgNO_3$.
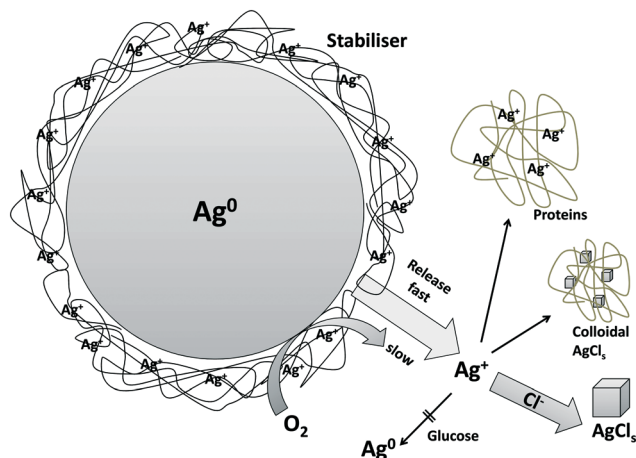

Fig. 5 Graphical representation of our conclusions (inspired by Loza *et al.*[74]).

For Scenedesmus we see an exception, the predicted value is in the twofold standard deviation of the experimental EC_{50}. This underestimation cannot be explained by water chemistry and is probably attributed to the test organisms.

4 Conclusions

Here we report for the first time the effect of test media composition on speciation of the OECD reference silver nanomaterial NM-300K for a wide variety of media and its influence on (eco)toxicological effects. This material was used in many studies on nanosafety due to its unique stability proper-

ties. For this purpose we determined the silver release of this material in toxicological test media containing different ligands such as chloride, amino acids and proteins. The media were chosen to cover organisms in the aquatic and terrestrial environments (algae, crustaceans, aquatic plants and bacteria). Additionally, a cell growth medium was also part of the study to account for direct exposure to higher organisms. The release of Ag^+ was numerically predicted and validated by experimental speciation methods, in particular MF and UC.

Since the release of Ag^+ from AgNPs in the toxicological tests is one important factor determining the bioavailability for the tested organisms, release experiments were conducted in the time frame of the tests. The results show the controlling role of chloride and silver binding proteins in the behavior of all AgNPs in biological media, which was reported for other AgNPs by several groups, Liu *et al.* among others.[5,13,36,82] Our conclusions are graphically summarised in Fig. 5.

The presented data for NM-300K nanoparticles suggest the important role of their coating, which causes high dispersion stability and also high redox stability. The initial release of Ag^+ is most likely due to Ag^+ already present in the stock dispersion within the coating layer on the NP surface.

Dissolved oxygen initiates only long-term release of Ag^+. Hence, the influence of redox reactions plays a minor role in the course of short-term toxicological tests. As a realistic approach for the prediction of Ag speciation in ecotoxicological media, it has been proven correct to use the initial chemical conditions of the AgNP stock dispersion determined by experimental speciation as a starting point. Using this origin pattern for the speciation calculations predicted correctly the experimental findings for NM-300K by UC or MF, when not allowing for possible redox processes in the calculations. Allowing for redox-reactions in our speciation calculations strongly overestimated the influence of the media components (dissolved oxygen) or the reductive components (glucose and ammonium).

The use of both methods MF and UC for the experimental speciation of *e.g.* silver proved to be complementary. This complementary approach served here as an experimental starting point to verify equilibrium data for ion binding to macromolecules to model the fate of nanoparticles and ions in complex media. However, in order to allow for a more reliable hazard assessment and predictions of the long-term dissolution behavior of AgNPs, additional studies are required in a several month timescale, especially when investigating the aging effects in the soil like Hoppe *et al.*[83] Comparing the toxic effects of the AgNP NM-300K and $AgNO_3$ in the here studied test systems led to the conclusion that in the relatively short time frame of the tests, the observed toxic effects of AgNPs were caused by a proportion of Ag^+ that was already present in the stock dispersion before the beginning of the tests and not from further release due to later oxidation processes. In the case of bacteria *Arthrobacter g.* solubility equilibrium is reached in the range of EC_{50} and colloidal precipitates contribute to the toxic effect. This realistic approach could prove to be a powerful tool for the evaluation of toxicity tests of nanoparticles and for the prediction of the speciation and bioavailability of nanoparticles in toxicological test media.

Acknowledgements

References

1 S. Chernousova and M. Epple, *Angew. Chem., Int. Ed.*, 2013, **52**, 1636–1653.

2 E. Navarro, B. Wagner, N. Odzak, L. Sigg and R. Behra, *Environ. Sci. Technol.*, 2015, **49**, 8041–8047.

3 E. Navarro, A. Baun, R. Behra, N. Hartmann, J. Filser, A.-J. Miao, A. Quigg, P. Santschi and L. Sigg, *Ecotoxicology*, 2008, **17**, 372–386.

4 O. Choi, T. E. Clevenger, B. Deng, R. Y. Surampalli, L. Ross Jr. and Z. Hu, *Water Res.*, 2009, **43**, 1879–1886.

5 J. Liu, D. A. Sonshine, S. Shervani and R. H. Hurt, *ACS Nano*, 2010, **4**, 6903–6913.

6 R. Ma, C. Levard, S. M. Marinakos, Y. Cheng, J. Liu, F. M. Michel, G. E. Brown and G. V. Lowry, *Environ. Sci. Technol.*, 2012, **46**, 752–759.

7 W. Zhang, Y. Yao, N. Sullivan and Y. Chen, *Environ. Sci. Technol.*, 2011, **45**, 4422–4428.

8 J. M. Unrine, B. P. Colman, A. J. Bone, A. P. Gondikas and C. W. Matson, *Environ. Sci. Technol.*, 2012, **46**, 6915–6924.

9 B. C. Reinsch, C. Levard, Z. Li, R. Ma, A. Wise, K. B. Gregory, G. E. Brown and G. V. Lowry, *Environ. Sci. Technol.*, 2012, **46**, 6992–7000.

10 S. Kittler, C. Greulich, J. Diendorf, M. Köller and M. Epple, *Chem. Mater.*, 2010, **22**, 4548–4554.

11 H. Hagendorfer, R. Kaegi, M. Parlinska, B. Sinnet, C. Ludwig and A. Ulrich, *Anal. Chem.*, 2012, **84**, 2678–2685.

12 J. Dobias and R. Bernier-Latmani, *Environ. Sci. Technol.*, 2013, **47**, 4140–4146.

13 J. Liu, Z. Wang, F. D. Liu, A. B. Kane and R. H. Hurt, *ACS Nano*, 2012, **6**, 9887–9899.

14 N. F. Adegboyega, V. K. Sharma, K. Siskova, R. Zboril, M. Sohn, B. J. Schultz and S. Banerjee, *Environ. Sci. Technol.*, 2013, **47**, 757–764.

15 V. Amendola and M. Meneghetti, *J. Phys. Chem. C*, 2009, **113**, 4277–4285.

16 A. Nogowski, F. Babick, P. Fiala and M. Stintz, *PARTEC*, Nürnberg, April, 2013.

17 D. M. Mitrano, A. Barber, A. Bednar, P. Westerhoff, C. P. Higgins and J. F. Ranville, *J. Anal. At. Spectrom.*, 2012, **27**, 1131–1142.

18 M. D. Montaño, J. W. Olesik, A. G. Barber, K. Challis and J. F. Ranville, *Anal. Bioanal. Chem.*, 2016, **408**, 5053–5074.

19 G. Koopmans, T. Hiemstra, I. Regelink, B. Molleman and R. Comans, *J. Chromatogr. A*, 2015, **1392**, 100–109.

20 C. L. Doolette, M. J. McLaughlin, J. K. Kirby, D. J. Batstone, H. H. Harris, H. Ge and G. Cornelis, *Chem. Cent. J.*, 2013, **7**, 46.

21 R. Kaegi, A. Voegelin, B. Sinnet, S. Zuleeg, H. Siegrist and M. Burkhardt, *Sci. Total Environ.*, 2015, **535**, 20–27.

22 H. Ratte, *Environ. Toxicol. Chem.*, 1999, **18**, 89–108.

23 B. Naumann, M. Eberius and K.-J. Appenroth, *J. Plant Physiol.*, 2007, **164**, 1656–1664.

24 D.-Y. Lee, C. Fortin and P. G. Campbell, *Aquat. Toxicol.*, 2005, **75**, 127–135.

25 P. Dibrov, J. Dzioba, K. K. Gosink and C. C. Häse, *Antimicrob. Agents Chemother.*, 2002, **46**, 2668–2670.

26 E. Navarro, F. Piccapietra, B. Wagner, F. Marconi, R. Kaegi, N. Odzak, L. Sigg and R. Behra, *Environ. Sci. Technol.*, 2008, **42**, 8959–8964.

27 E. J. Gubbins, L. C. Batty and J. R. Lead, *Environ. Pollut.*, 2011, **159**, 1551–1559.

28 A. M. E. Badawy, R. G. Silva, B. Morris, K. G. Scheckel, M. T. Suidan and T. M. Tolaymat, *Environ. Sci. Technol.*, 2011, **45**, 283–287.

29 F. Broggi, J. Ponti, G. Giudetti, V. Franchini, V. Stone, C. P. Garcia and F. Rossi, *BioNanoMaterials*, 2013, **14**, 49–60.

30 M. Engelke, J. Köser, S. Hackmann, H. Zhang, L. Mädler and J. Filser, *Environ. Toxicol. Chem.*, 2014, **33**, 1142–1147.

31 D. Voelker, K. Schlich, L. Hohndorf, W. Koch, U. Kuehnen, C. Polleichtner, C. Kussatz and K. Hund-Rinke, *Environ. Res.*, 2015, **140**, 661–672.

32 J. P. Gustafsson, *Visual MINTEQ ver. 3.0*, Department of Land and Water Resources Engineering, KTH, Sweden, 2010.

33 J. C. Westall, J. L. Zachary and F. M. M. Morel, *MINEQL, A Computer Program for the Calculation of Chemical Equilibrium Composition of Aqueous Systems; Technical Note 18*, R. M. Parsons Laboratory, Massachusetts Institute of Technology, Cambridge, MA, 1976.

34 W. Schecher and D. McAvoy, *MINEQL+: A Chemical Equilibrium Program for Personal Computers, Ver 3.01. Environmental Research Software*, Hallowell, ME, USA, 1994.

35 D. Parkhurst and C. Appelo, *PHREEQC*, U.S. Geological Survey, 2010, http://wwwbrr.cr.usgs.gov/projects/GWC_coupled/phreeqc/index.html, (accessed January 2017).

36 J. Liu and R. H. Hurt, *Environ. Sci. Technol.*, 2010, **44**, 2169–2175.

37 C. Fortin and P. Campbell, *Environ. Toxicol. Chem.*, 2000, **19**, 2769–2778.

38 J. R. Reinfelder and S. I. Chang, *Environ. Sci. Technol.*, 1999, **33**, 1860–1863.

39 X. Jin, M. Li, J. Wang, C. Marambio-Jones, F. Peng, X. Huang, R. Damoiseaux and E. Van Hoek, *Environ. Sci. Technol.*, 2010, **44**, 7321–7328.

40 C. Levard, E. M. Hotze, G. V. Lowry and G. E. Brown, *Environ. Sci. Technol.*, 2012, **46**, 6900–6914.

41 C. Klein, S. Comero, B. Stahlmecke, J. Romazanov, T. Kuhlbusch, E. V. Doren, P.-J. D. Temmerman, J. Mast, P. Wick, H. Krug, G. Locoro, K. Hund-Rinke, W. Kördel, S. Friedrichs, G. Maier, J. Werner, T. Linsinger and B. Gawlik, *NM-Series of Representative Manufactured Nanomaterials - NM-300 Silver Characterisation, Stability, Homogeneity, EUR*

This journal is © The Royal Society of Chemistry 2017

Environ. Sci.: Nano, 2017, **4**, 1470–1483 | 1481

24693 EN - Joint Research Centre - Institute for Health and Consumer Protection Technical Report EUR - Scientific and Technical Research series - ISSN 1018-5593, ISBN 978-92-79-19068-1, 2011.

42 EU NanoSafety Cluster, 2017, www.nanosafetycluster.eu, (accessed January 2017).

43 *DaNa 2.0, Information about nanomaterials and their safety assessment, projects*, http://nanopartikel.info/en/projects, (accessed January 2017).

44 J. Köser, M. Engelke, A. Kück, E. Lesnikov, J. Arning, J. Thöming and J. Filser, *Abschätzung der Umweltgefährdung durch Silber-Nanomaterialien: Vom chemischen Partikel bis zum technischen Produkt (UMSICHT), Abschlussbericht Universität Bremen, Germany*, 2013, http://www.umsicht.uni-bremen.de/ Abschlussberichte Partner/Abschlussbericht_Uni_HB_2013-12-16_public.pdf, (accessed January 2017).

45 A. Lüdecke, C. Polleichtner and D. Völker, *Abschätzung der Umweltgefährdung durch Silber-Nanomaterialien: Vom chemischen Partikel bis zum technischen Produkt (UMSICHT), Schlussbericht Umweltbundesamt, Berlin & Dessau-Roßlau, Germany*, 2014, http://www.umsicht.uni-bremen.de/ Abschlussberichte Partner/UBA Gesamtschlussbericht_ UMSICHT_final mit Anlagen 1–3.pdf, (accessed January 2017).

46 P. S. Tourinho, C. A. van Gestel, K. Jurkschat, A. M. Soares and S. Loureiro, *Environ. Pollut.*, 2015, **205**, 170–177.

47 B. Welz and M. Sperling, *Atomabsorptionsspektrometrie*, Wiley-VCH, Weinheim [u.a.], 4th edn, 1997.

48 Deutsches Institut für Normung e.V., *DIN ISO 11466 - Bodenbeschaffenheit - Extraktion in Königswasser löslicher Spurenelemente (ISO 11466:1995)*, 1995.

49 D. K. Wilkins, S. B. Grimshaw, V. Receveur, C. M. Dobson, J. A. Jones and L. J. Smith, *Biochemistry*, 1999, **38**, 16424–16431.

50 *CRC Handbook of Chemistry and Physics*, ed. W. M. Haynes, CRC Press, Boca Raton, FL, 93rd edn, 2012, p. 2664.

51 A. Pingoud and C. Urbanke, *Arbeitsmethoden der Biochemie*, de Gruyter, Berlin [u.a.], 1997.

52 J. Baumann, Y. Sakka, C. Bertrand, J. Köser and J. Filser, *Environ. Sci. Pollut. Res.*, 2014, **21**, 2201–2213.

53 OECD, *OECD Guidelines for the Testing of Chemicals, Section 2: Effects on Biotic Systems, Test No. 201: Freshwater Alga and Cyanobacteria, Growth Inhibition Test*, 2011, http://www.oecd-ilibrary.org/environment/test-no-201-alga-growth-inhibition-test_9789264069923-en, (accessed January 2017).

54 OECD, *OECD Guidelines for the Testing of Chemicals, Section 2: Effects on Biotic Systems, Test No. 202: Daphnia sp. Acute Immobilisation Test*, 2004, http://www.oecd-ilibrary.org/content/book/9789264069947-en, (accessed January 2017).

55 OECD, *OECD Guidelines for the Testing of Chemicals, Section 2: Effects on Biotic Systems, Test No. 221: Lemna sp. Growth Inhibition Test*, 2006, http://www.oecd-ilibrary.org/

environment/test-no-221-lemna-sp-growth-inhabition-test_9789264016194-en, (accessed January 2017).

56 M. Matzke, S. Stolte, K. Thiele, T. Juffernholz, J. Arning, J. Ranke and B. Jastorff, *Green Chem.*, 2007, **9**, 1198–1207.

57 L. Grimme and N. Boardman, *Biochem. Biophys. Res. Commun.*, 1972, **49**, 1617–1623.

58 H. Neumann-Hensel and K. Melbye, *J. Soils Sediments*, 2006, **6**, 201–207.

59 Deutsches Institut für Normung e.V., *DIN Richtlinie 38412 Teil 48 - Deutsche Einheitsverfahren zur Wasser-, Abwasser- und Schlammuntersuchung - Testverfahren mit Wasserorganismen (Gruppe L) - Teil 18: Arthrobacter globiformis-Kontakttest für kontaminierte Feststoffe*, 2002.

60 J. Arning, M. Matzke, S. Stolte, F. Nehen, U. Bottin-Weber, A. Böschen, S. Abdulkarim, B. Jastorff and J. Ranke, *Chem. Res. Toxicol.*, 2009, **22**, 1954–1961.

61 D. Parkhurst, *PHREEQCi v3.3.7-11094*, 2016, http://wwwbrr.cr.usgs.gov/projects/GWC_coupled/phreeqci/, (accessed January 2017).

62 N. W. Adams and J. R. Kramer, *Aquat. Geochem.*, 1999, **5**, 1–11.

63 R. M. Smith, *NIST Standard Reference Database 46 - NIST Critically Selected Stability Constants of Metal Complexes: Version 8.0*, 2004, http://www.nist.gov/srd/nist46, (accessed January 2017).

64 G. Berthon, *Pure Appl. Chem.*, 1995, **67**, 1117–1240.

65 R. N. Goldberg, N. Kishore and R. M. Lennen, *J. Phys. Chem. Ref. Data*, 2002, **31**, 231–370.

66 C. M. Wood, M. D. McDonald, P. Walker, M. Grosell, J. F. Barimo, R. C. Playle and P. J. Walsh, *Aquat. Toxicol.*, 2004, **70**, 137–157.

67 X.-C. Shen, H. Liang, J.-H. Guo, C. Song, X.-W. He and Y.-Z. Yuan, *J. Inorg. Biochem.*, 2003, **95**, 124–130.

68 X. Zhao, R. Liu, Y. Teng and X. Liu, *Sci. Total Environ.*, 2011, **409**, 892–897.

69 A. Marty, M. Boiret and M. Deumie, *J. Chem. Educ.*, 1986, **63**, 365.

70 I. Rombouts, B. Lagrain, K. A. Scherf, M. A. Lambrecht, P. Koehler and J. A. Delcour, *Sci. Rep.*, 2015, **5**, 12210.

71 P. Alexander and L. D. G. Hamilton, *Arch. Biochem. Biophys.*, 1960, **88**, 128–135.

72 R. K. Thauer, K. Jungermann and K. Decker, *Bacteriol. Rev.*, 1977, **41**, 100–180.

73 S. Ramachandran, P. Fontanille, A. Pandey and C. Larroche, *Food Technol. Biotechnol.*, 2006, **44**, 185–195.

74 K. Loza, J. Diendorf, C. Sengstock, L. Ruiz-Gonzalez, J. M. Gonzalez-Calbet, M. Vallet-Regi, M. Köller and M. Epple, *J. Mater. Chem. B*, 2014, **2**, 1634–1643.

75 X. Li and J. J. Lenhart, *Environ. Sci. Technol.*, 2012, **46**, 5378–5386.

76 Universal Protein Resource, *Serum albumin (BSA), P02769 (ALBU_BOVIN)*, 2013, http://www.uniprot.org/uniprot/P02769, (accessed January 2017).

77 Organotechnie S.A.S., *Technical Data Sheets for Yeast Extract 19512 and Casein Peptones E1 19564, N1 19516, Plus 19544*, 2017, http://www.organotechnie.com/products/yeast-extract/

1482 | *Environ. Sci.: Nano*, 2017, **4**, 1470–1483

This journal is © The Royal Society of Chemistry 2017

and http://www.organotechnie.com/products/#slidefamily81, (accessed January 2017).

78 D. Zirkler, F. Lang and M. Kaupenjohann, *Colloids Surf., A*, 2012, **399**, 35–40.

79 X. Li, J. J. Lenhart and H. W. Walker, *Langmuir*, 2010, **26**, 16690–16698.

80 Z. Khan, J. I. Hussain, S. Kumar, A. A. Hashmi and M. A. Malik, *J. Biomater. Nanobiotechnol.*, 2011, **2**, 390–399.

81 K. Loza, C. Sengstock, S. Chernousova, M. Köller and M. Epple, *RSC Adv.*, 2014, **4**, 35290–35297.

82 J. Liu, K. G. Pennell and R. H. Hurt, *Environ. Sci. Technol.*, 2011, **45**, 7345–7353.

83 M. Hoppe, R. Mikutta, J. Utermann, W. Duijnisveld, S. Kaufhold, C. F. Stange and G. Guggenberger, *Eur. J. Soil Sci.*, 2015, **66**, 898–909.

This journal is © The Royal Society of Chemistry 2017

Environ. Sci.: Nano, 2017, **4**, 1470–1483 | **1483**